

## Research Article

# Photocatalytic Degradation of Methylene Blue under UV Light Irradiation on Prepared Carbonaceous TiO<sub>2</sub>

Zatil Amali Che Ramli,<sup>1</sup> Nilofar Asim,<sup>1</sup> Wan N. R. W. Isahak,<sup>2</sup> Zeynab Emdadi,<sup>1</sup>  
Norasikin Ahmad-Ludin,<sup>1</sup> M. Ambar Yarmo,<sup>2</sup> and K. Sopian<sup>1</sup>

<sup>1</sup> Solar Energy Research Institute, Universiti Kebangsaan Malaysia, 43600 Bangi, Selangor, Malaysia

<sup>2</sup> School of Chemical Science & Food Technology, Faculty of Science and Technology, Universiti Kebangsaan Malaysia, 43600 Bangi, Selangor, Malaysia

Correspondence should be addressed to Nilofar Asim; [asimnilofar@gmail.com](mailto:asimnilofar@gmail.com)

Received 6 February 2014; Accepted 7 May 2014; Published 11 June 2014

Academic Editor: Liqiang Jing

Copyright © 2014 Zatil Amali Che Ramli et al. This is an open access article distributed under the Creative Commons Attribution License, which permits unrestricted use, distribution, and reproduction in any medium, provided the original work is properly cited.

This study involves the investigation of altering the photocatalytic activity of TiO<sub>2</sub> using composite materials. Three different forms of modified TiO<sub>2</sub>, namely, TiO<sub>2</sub>/activated carbon (AC), TiO<sub>2</sub>/carbon (C), and TiO<sub>2</sub>/PANi, were compared. The TiO<sub>2</sub>/carbon composite was obtained by pyrolysis of TiO<sub>2</sub>/PANi prepared by in situ polymerization method, while the TiO<sub>2</sub>/activated carbon (TiO<sub>2</sub>/AC) was obtained after treating TiO<sub>2</sub>/carbon with 1.0 M KOH solution, followed by calcination at a temperature of 450°C. X-ray powder diffraction (XRD), transmission electron microscopy (TEM), Fourier transform infrared (FTIR), thermogravimetric analysis (TG-DTA), Brunauer-Emmet-Teller (BET), and UV-Vis spectroscopy were used to characterize and evaluate the prepared samples. The specific surface area was determined to be in the following order: TiO<sub>2</sub>/AC > TiO<sub>2</sub>/C > TiO<sub>2</sub>/PANi > TiO<sub>2</sub> (179 > 134 > 54 > 9 m<sup>2</sup> g<sup>-1</sup>). The evaluation of photocatalytic performance for the degradation of methylene blue under UV light irradiation was also of the same order, with 98 > 84.7 > 69% conversion rate, which is likely to be attributed to the porosity and synergistic effect in the prepared samples.

## 1. Introduction

Currently, the rapid industrialization in developing countries has begun to introduce harmful organic pollutants into the water supply. These effluents are also sourced from the textile industry that consumes a large quantity of water in the process of dyeing and washing of fabrics and the release of huge quantities of dyes [1]. Therefore, the development of inexpensive and green methods to treat and purify contaminated water has been the focal subject in technological developments. Among many strategies, photocatalysis is regarded as the most viable one, especially for treatment of contaminants, due to its usage of sunlight to decompose organic pollutants [2–4]. Titanium dioxide or titania (TiO<sub>2</sub>) acts as an agent in this process [5, 6]. However, TiO<sub>2</sub> is not without its drawback in the context of photocatalysis, such as its high band gap energy 3.2 eV for anatase [7], the limitation of photo response only under UV light region, and its high

rate of electron and hole recombination. Attempts to address these problems involve doping, nonmetallic elements doping, surface modification, forming composites with narrow semiconductors, using semiconductor polymer as support, and coating with carbon layers to improve and enhance the photocatalytic activity of titanium dioxide.

Current literature shows that activated carbon is gaining attention as it is capable of modifying TiO<sub>2</sub> photocatalyst. The work in [8–12] showed that this enhancement is caused by porous structure of activated carbon, which provides a large surface area for photoactive TiO<sub>2</sub> particle.

The work in [8, 13–15] found the synergistic effect of the mixture of TiO<sub>2</sub> with activated carbon (AC). The improvement of TiO<sub>2</sub>/AC composite was explained by the high adsorption of the impurities on the surface of activated carbon and their transfer to the TiO<sub>2</sub> surface. In this study, carbonaceous TiO<sub>2</sub>, namely, TiO<sub>2</sub>/activated carbon (AC), TiO<sub>2</sub>/carbon (C), and TiO<sub>2</sub>/PANi were prepared and

evaluated for photocatalytic performance for degradation of methylene blue under UV light irradiation. The carbon and activated carbon/TiO<sub>2</sub> were synthesized using polyaniline (PANi) as its carbon source.

## 2. Experimental and Characterizations

**2.1. Preparation of TiO<sub>2</sub>/Polyaniline and TiO<sub>2</sub>/Carbon.** TiO<sub>2</sub>/polyaniline (TiO<sub>2</sub>/PANi) was synthesized using TiO<sub>2</sub> (Sigma Aldrich, 99.9% purity) and aniline hydrochloride (Sigma Aldrich, 99.95%). In order to synthesize TiO<sub>2</sub>/PANi, 0.2 mol cm<sup>-3</sup> aniline hydrochloride solution was prepared by adding 259 mg aniline hydrochloride to 5 mL deionized water and was vigorously stirred for 10 minutes at a temperature of 60°C. TiO<sub>2</sub> powder, with various percentages (5%, 10% and 15%), is added to aniline hydrochloride solution being prepared previously. 0.25 mol cm<sup>-3</sup> ammonium peroxydisulphate solution was prepared by adding 571 mg ammonium peroxydisulphate (Sigma Aldrich, 98% reagent grade) in 5 mL deionized water. While the mixture above was being stirred, the prepared ammonium peroxydisulphate solution was added to the mixture and was stirred for an additional 10 minutes. The polymerization was completed in about 10 minutes. The solution was then left to dry at room temperature for 48 hours. The precipitate powder was then centrifuged and washed with absolute ethanol, followed by distilled water in order to remove unreacted aniline monomer and its corresponding by-products. The product (TiO<sub>2</sub>/PANi) was dried at 65°C for 24 h. The composite that was the result of the process was labeled as TiO<sub>2</sub>/PANi. The product was then pyrolyzed at a temperature of 450°C for 1 hour in nitrogen flow at a heating rate of 10°C min<sup>-1</sup> to produce titania/carbon (TiO<sub>2</sub>/C).

**2.2. Chemical Activation of TiO<sub>2</sub>/Carbon.** In order to produce porous carbon or the so-called activated carbon, the TiO<sub>2</sub>/C was treated with 1.0 M KOH solution. About 0.3 g TiO<sub>2</sub>/C was mixed with 2.5 mL 1.0 M KOH solution. The mixture was then heated at a temperature of 450°C under nitrogen gas flow for 1 hour. Then the treated sample was washed with deionized water until it was neutral and dried overnight at a temperature of 100°C and was labeled TiO<sub>2</sub>/AC. Since the early photocatalytic performance tests demonstrated better result for the TiO<sub>2</sub>/AC prepared from 15% TiO<sub>2</sub>/PANi, the characterization was done for 15% TiO<sub>2</sub>/PANi and the resulting TiO<sub>2</sub>/C and TiO<sub>2</sub>/AC (hereafter denoted as TiO<sub>2</sub>/PANi, TiO<sub>2</sub>/C, and TiO<sub>2</sub>/AC, resp.).

**2.3. Characterizations.** The functionality groups of the samples were determined using FTIR spectra. The morphology and structure of the samples were determined by field emission scanning electron microscope (FESEM, ZEISS Supra VP55) and transmission electron microscope (JEOL JEM-2100). The specific surface area, pore size, pore volume, and pore diameter of the samples were determined by Brunauer-Emmet-Teller (BET) method [16] using a nitrogen adsorption instrument (Micrometcs ASAP 2010). The samples were degassed at 100°C for 24 hours prior to the analysis. Pore size

distribution was calculated from the adsorption desorption of the isotherms using the Barret-Joyner-Halenda (BJH) model [17], while the crystallinity of the samples was analyzed using Bruker DB-advance X-ray diffractometer (XRD). The analyses were done under the setting of Cu K $\alpha$  radiation at 2 theta, ranging from 10° to 80° for a 1-gram sample. The particle size of the sample was calculated by applying Scherrer's equation. Thermal gravimetric analysis (TGA) with a simultaneous TGA-DTG system (model: Mettler Toledo) has been used for investigation of thermal stability of samples. To reduce the influence of the sample quantity on the analyses, 5 ± 0.2 mg of each sample was used in each analysis with a constant nitrogen (N<sub>2</sub>) flow 50.0 mL min<sup>-1</sup> maintained throughout the entire process. To minimize possible differences in the moisture content between samples, all TGA samples were equilibrated at 50°C for 5 min before being heated to 700°C at a ramping rate of 5°C min<sup>-1</sup>.

For investigation of prepared samples recyclability, the used catalyst was separated from reaction mixture by filtration. After that, it is washed with distilled water several times and dried in oven to be reused for next reaction cycle. Then they were used for subsequent cycles under similar reaction conditions as carried out by fresh catalyst.

**2.4. Photocatalytic Experimental.** The photocatalytic activities of the samples were evaluated via the photocatalytic oxidation of methylene blue (MB) under UV light irradiation. A 15 watt UV bench lamp was used as a light source. Since the photocatalytic test took into account different MB concentrations (0.05, 0.1, and 0.15 mM) and different irradiation times, it showed better results for 0.05 mM and 90 minutes, respectively, and was selected as the test condition (see Section 3.2).

Prior to illumination, 20 mg photocatalyst was added to the MB solution (20 mL, 0.05 mM). The solution was stirred in the dark for 30 minutes in order to reach MB absorption-desorption equilibrium, which will then allow for the commencement of the photocatalytic reaction. The photocatalyst will then be exposed to the UV lamp for 90 minutes in room temperature. The results after this time period will be evaluated after 90 minutes.

The degradation efficiency of MB was analyzed using UV-Vis spectrometer. Peaks were observed to be present between 600 and 700 nm and were assigned as the absorption of the  $\pi$ -system [18], which was indicative of the degradation of MB. According to Beer-Lambert Law, MB's concentration is directly proportional to its absorbance. This makes it possible to determine the oxidation efficiency of MB using the following equation:

$$R = \frac{(C_o - C_t)}{C_o} \times 100\%, \quad (1)$$

where  $C_o$  is the initial concentration of MB solution and  $C_t$  is concentration of MB during irradiation.

### 3. Results and Discussions

The existence of polyaniline on the TiO<sub>2</sub> surface particle was verified by IR spectra. The characteristic bands of TiO<sub>2</sub>, polyaniline (made in the same way for comparison purpose only), TiO<sub>2</sub>/PANi, and TiO<sub>2</sub>/AC are shown in Figures 1(a), 1(b), 1(c), and 1(d), respectively. The FTIR spectrum of polyaniline was clearly observed in TiO<sub>2</sub>/PANi sample. The spectra display the two bands at 1490 and 1585 cm<sup>-1</sup>, which were assigned to benzenoid and quinoid rings. The band at 1300 cm<sup>-1</sup> is related to C–N stretching of a secondary aromatic amine, while the band at 1140 cm<sup>-1</sup> is attributed to the vibration mode of the polymer. These bands reveal the existence of PANi in the synthesized TiO<sub>2</sub>/PANi sample. In TiO<sub>2</sub> and TiO<sub>2</sub>/AC spectra, peaks around 3400 cm<sup>-1</sup> were assigned to –OH stretching, while those at 1600 cm<sup>-1</sup> were assigned to –OH vibration. These peaks can be attributed to the adsorbed water from the environment.

The morphologies and size of the prepared nanoparticles were studied by variable pressure scanning electron microscope (VPSEM) and transmission electron microscopy (TEM) (Figures 2 and 3).

From the TEM image of Figure 3(a), it was shown that bare TiO<sub>2</sub> particles are uniform in shape, with sizes ranging from 25 to 30 nm. Figure 3(b) shows TiO<sub>2</sub>/PANi composite, where the sizes range from 30 to 40 nm. Both TEM and FESEM photographs show that there is no significant difference of particle size of the samples TiO<sub>2</sub>/C and TiO<sub>2</sub>/AC (before and after chemical activation of KOH solution) (40–80 nm). This agrees with previous studies, which reported that the sintering effect did not occur for TiO<sub>2</sub>/carbon after being heated at temperatures below 700°C [19].

The XRD patterns of the prepared samples were shown in Figure 4. The main diffraction peaks were at 25.3°, 37.8°, 48°, 54°, and 62.6°, assigned to the diffraction planes of (1 0 1), (0 0 4), (2 0 0), (1 0 5), and (2 0 4) for anatase (JCPDS number 021-1272), respectively. Other crystal phases corresponding to the peaks at 27.4 and 36.1° were assigned to the diffraction peaks of (1 1 0) and (1 0 1) of rutile (JCPDS number 021-1276), respectively. The XRD patterns revealed the diffraction peaks of a mixture of anatase and rutile in the prepared samples, which is favorable for photocatalytic reactions [20–23]. XRD also showed that the preparation of TiO<sub>2</sub> composites did not affect the crystal structure of TiO<sub>2</sub>, but the peaks intensity became lower and its shape got wider, especially in the case of TiO<sub>2</sub>/PANi. This can be attributed to certain crystalline structure in PANi overlapping TiO<sub>2</sub> peaks, but this effect is less pronounced in TiO<sub>2</sub>/C and TiO<sub>2</sub>/AC. The anatase content ( $f(A)$ ) was determined from the integrated intensity of the anatase diffraction line (1 0 1),  $I_A$ , and that of the rutile diffraction line (1 1 0),  $I_R$ , using the following equation [24] and the results are listed in Table 1:

$$f(A) = \frac{1}{1 + 12.6(I_A/I_R)}. \quad (2)$$

The  $f(A)$  values showed that the rutile phase is dominant in all of the prepared samples. Besides that, the crystallite size of the samples was calculated by applying the Scherrer equation on the plane (101) diffraction peak of anatase and

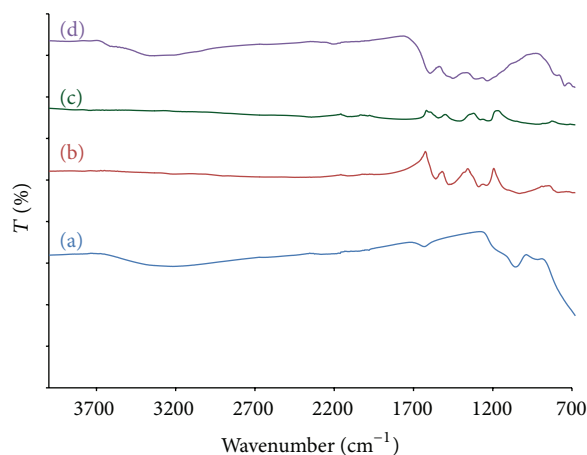


FIGURE 1: FTIR spectra of (a) TiO<sub>2</sub>, (b) Polyaniline, (c) TiO<sub>2</sub>/PANi, and (d) TiO<sub>2</sub>/AC, respectively.

(110) diffraction peak of rutile, as listed in Table 1. The BET surface area, pore size, micropore area, and volumes are listed in Table 1 as well. The results showed that the specific surface area adhered to the following order: TiO<sub>2</sub>/AC > TiO<sub>2</sub>/C > TiO<sub>2</sub>/PANi > TiO<sub>2</sub> (179 > 134 > 54 > 9 m<sup>2</sup> g<sup>-1</sup>). This suggests that the characteristics of the composited catalyst were enhanced, as it provided more active sites for photocatalytic reactions to take place.

The thermal stability of the prepared TiO<sub>2</sub>/PANi and TiO<sub>2</sub>/AC was investigated and the TG-DTA analysis results are shown in Figure 5. The first weight loss took place in the range of temperature 50–120°C for TiO<sub>2</sub>/PANi, which is 6.5% decrease from the original weight. The weight loss is due to the loss of moisture or water content, the evaporation of solvents such as ethanol and small molecules from the polymer matrix [25]. The second loss was determined at temperatures between 310 and 700°C. During this step, the weight loss was attributed to the degradation of polyaniline main chain (about 54%) [26–28]. At a temperature of about 700°C, the PANi molecule was completely decomposed to carbon. The result showed that TiO<sub>2</sub>/AC has significantly improved thermal stabilities compared to TiO<sub>2</sub>/PANi.

**3.1. Evaluation of Photocatalytic Performance.** The degradation of methylene blue (MB) was used in this work in order to evaluate the photocatalytic activity of the prepared samples. The effect of different loading percentages of TiO<sub>2</sub> in activated carbon on photocatalytic activity has been investigated as well (Figure 6). The results showed that increasing the content of TiO<sub>2</sub> improves photocatalytic performances. From the tests, it was determined that the 15% TiO<sub>2</sub> loading was to be further tested.

It is known that the concentration of methylene blue influences the photocatalytic performance of the samples [29]. Therefore, in this study, the photocatalytic activity of TiO<sub>2</sub>/PANi and TiO<sub>2</sub>/AC (0.05 mM) using different concentrations of MB within 90 minutes irradiation time was studied. It can be seen that TiO<sub>2</sub>/activated carbon demonstrated

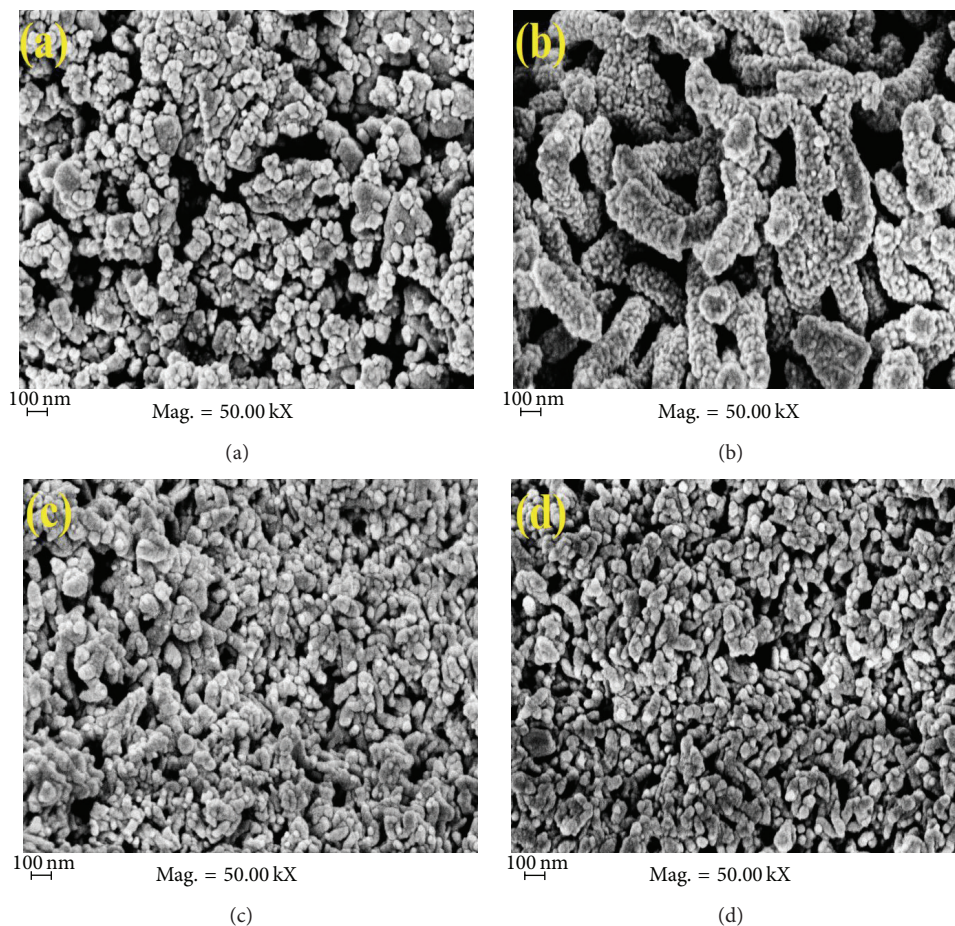


FIGURE 2: FESEM photographs of (a)  $\text{TiO}_2$  particles, (b)  $\text{TiO}_2/\text{PANi}$ , (c)  $\text{TiO}_2/\text{C}$ , and (d)  $\text{TiO}_2/\text{AC}$ , respectively.

TABLE 1: Texture properties of the  $\text{TiO}_2$ ,  $\text{TiO}_2/\text{PANi}$ ,  $\text{TiO}_2/\text{C}$ , and  $\text{TiO}_2/\text{AC}$  composites.

Physical properties	$\text{TiO}_2$	$\text{TiO}_2/\text{PANi}$	$\text{TiO}_2/\text{C}$	$\text{TiO}_2/\text{AC}$
Surface area ( $\text{m}^2/\text{g}$ )	8.55	53.73	134	178.57
Pore size (nm)	9.48	13.8	9.26	6.79
Micropore area ( $\text{m}^2/\text{g}$ )	3.34	8.22	29.33	76.62
Micropore volume ( $\text{cm}^3/\text{g}$ )	0.001	0.004	0.015	0.037
Crystallite size <sup>a</sup> (nm) anatase	25	14	—	11
Crystallite size <sup>a</sup> (nm) rutile	48	19	—	20
$f(A)$ <sup>b</sup>	0.135	0.061	0.087	0.092

<sup>a</sup> Calculated by applying Scherrer's equation.

<sup>b</sup> Anatase content calculated using (2).

superior photocatalytic activity for all different concentrations of MB (Figure 7).

The photocatalytic activity was also evaluated using irradiation time acting as its parameter (Figure 8). The result show rapid increase in MB degradation from 0 to 30 minutes which becomes slower after 30 minutes for both samples. The much higher MB degradation rate for  $\text{TiO}_2/\text{AC}$  proves its better performance compared to  $\text{TiO}_2/\text{PANi}$ .  $\text{TiO}_2/\text{AC}$  showed almost complete degradation of MB after 90 minutes of irradiation.

Figure 9 presents the result of the degradation of MB for bare  $\text{TiO}_2$ ,  $\text{TiO}_2/\text{PANi}$ ,  $\text{TiO}_2/\text{C}$ , and  $\text{TiO}_2/\text{AC}$ . The experiment was carried out in 90-minute irradiation, and the concentration of methylene blue was 0.05 mM for all samples. The degradation of MB without catalyst was used as a reference.

The results can be explained using texture properties of the prepared samples, as shown in Table 1. The specific surface area, micropore area, and volume adhered to the trend  $\text{TiO}_2/\text{AC} > \text{TiO}_2/\text{C} > \text{TiO}_2/\text{PANi} > \text{TiO}_2$ , which is

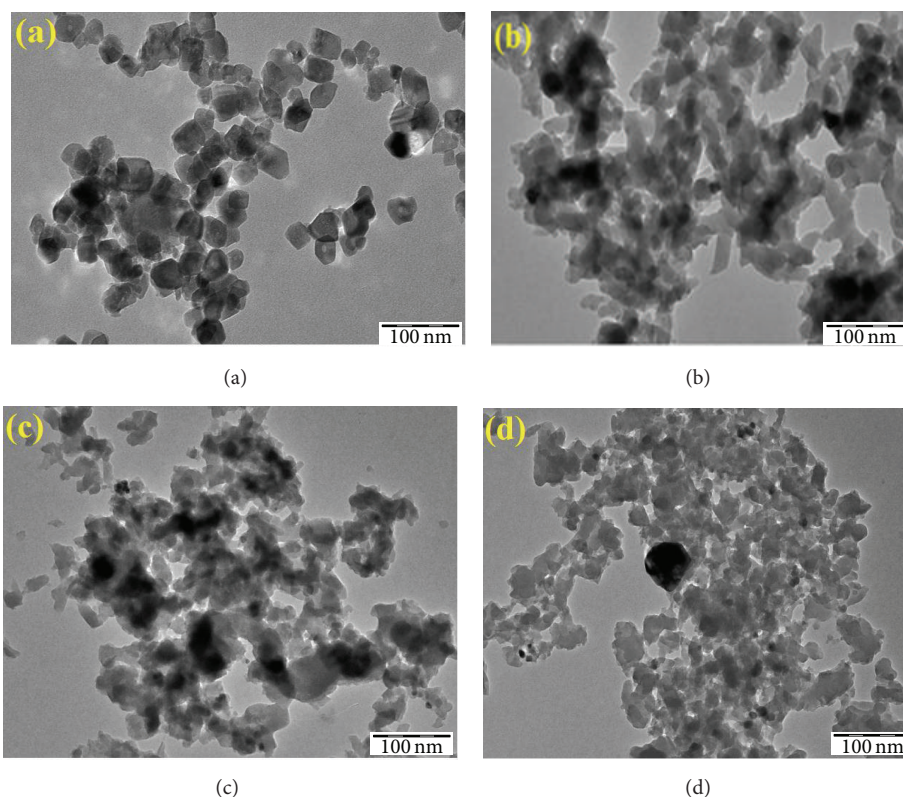


FIGURE 3: TEM photographs of (a)  $\text{TiO}_2$  particles, (b)  $\text{TiO}_2/\text{PANi}$ , (c)  $\text{TiO}_2/\text{C}$ , and (d)  $\text{TiO}_2/\text{AC}$ , respectively (magnification 45000x).

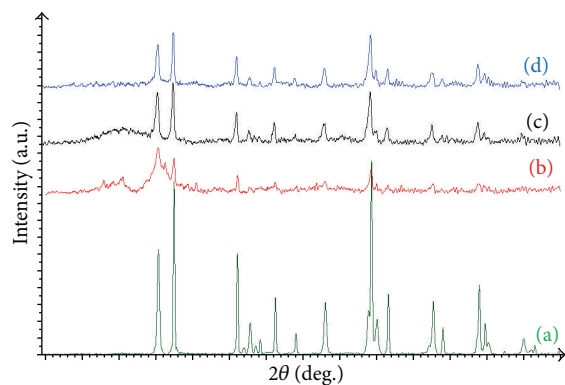


FIGURE 4: XRD patterns of samples. (a)  $\text{TiO}_2$  particles, (b)  $\text{TiO}_2/\text{PANi}$ , (c)  $\text{TiO}_2/\text{C}$ , and (d)  $\text{TiO}_2/\text{AC}$ , respectively.

similar to photocatalytic performance. This is attributed to the higher porosity of the activated carbon compared to others, which provide high adsorption capacity and more active sites for the reacting species during chemical reaction, which agrees with previous studies [8, 9, 19, 30–32]. It was noted that the surface area of  $\text{TiO}_2/\text{AC}$  is larger compared to the ones reported in the literature, which used polystyrene (PS) as a carbon source [33]. It also shows that PANi is a better source for the preparation of highly porous activated carbon.

On top of the synergistic effect for the mixture of  $\text{TiO}_2$  with activated carbon and highly porous structures, the

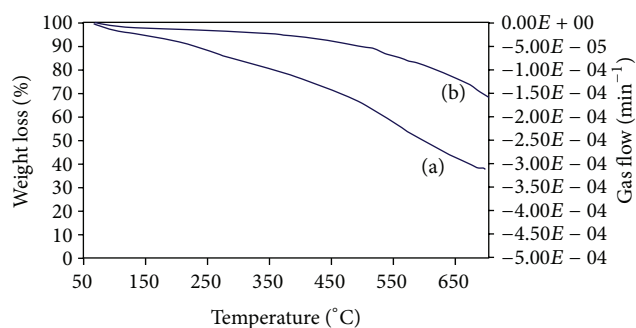


FIGURE 5: TGA thermogram analysis of (a)  $\text{TiO}_2/\text{PANi}$  and (b)  $\text{TiO}_2/\text{AC}$  composite.

high photocatalytic performance could be the result of the mixture of anatase and rutile phase of  $\text{TiO}_2$  in this work (Table 1). This can be explained by the synergistic effect between anatase and rutile in  $\text{TiO}_2$  particles that are approximately close to each other, thus enhancing the activity [34]. This finding is in agreement with other studies reporting that the photocatalytic activity was enhanced when anatase and rutile were mixed [34, 35].

**3.2. Recyclability of  $\text{TiO}_2/\text{AC}$ .** Recyclability test was carried out for  $\text{TiO}_2/\text{AC}$  to up to five cycles. The results are depicted in Figure 10, demonstrating good recyclability for the prepared composite.

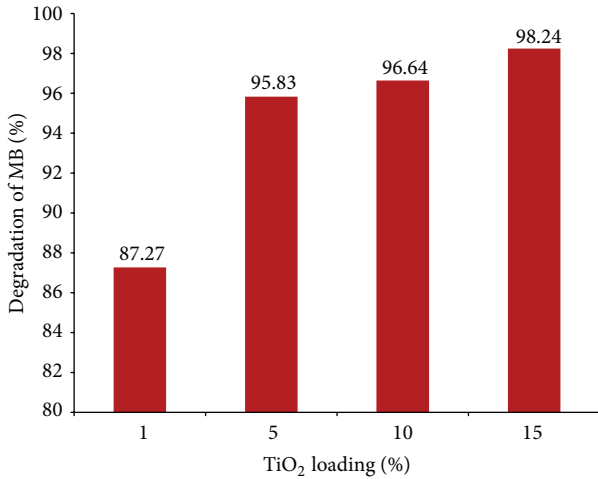


FIGURE 6: Effect of TiO<sub>2</sub> loading (%) on degradation of MB (under 90 minutes of UV light irradiation in room temperature).

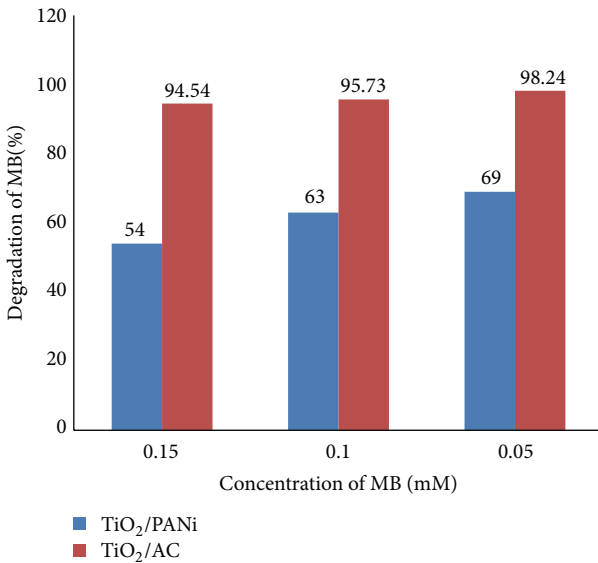


FIGURE 7: Effect of MB concentration on photocatalytic activity for TiO<sub>2</sub>/PANi and TiO<sub>2</sub>/AC.

**4. Conclusion**

Regarding the possibility of photocatalytic improvement using a composite of TiO<sub>2</sub>, a different form of modified TiO<sub>2</sub>, namely, TiO<sub>2</sub>/activated carbon (AC), TiO<sub>2</sub>/Carbon (C), and TiO<sub>2</sub>/PANi, were synthesized and characterized, and their catalytic performance have been studied. The effect of TiO<sub>2</sub> loading, irradiation time, and MB concentration has been studied. TiO<sub>2</sub>/AC showed the highest porosity and photocatalytic performance compared to other composites. On top of considering the synergistic effect for the mixture of TiO<sub>2</sub> with activated carbon and its high porosity, this high performance can also be attributed to the anatase and rutile mixture. Meanwhile, PANi demonstrated better AC source compared to previous works, and the recyclability

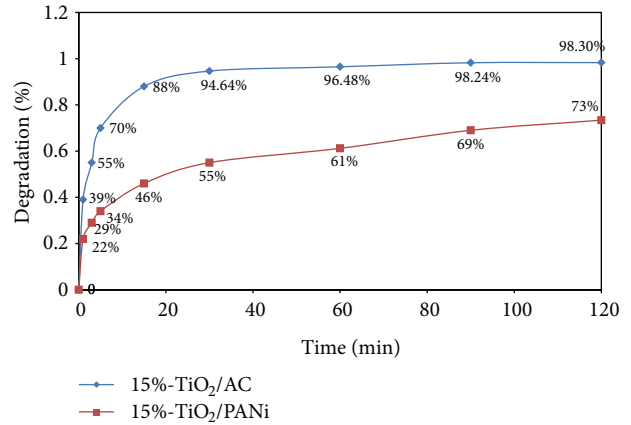


FIGURE 8: Photocatalytic activity: effect of irradiation time in degradation of MB.

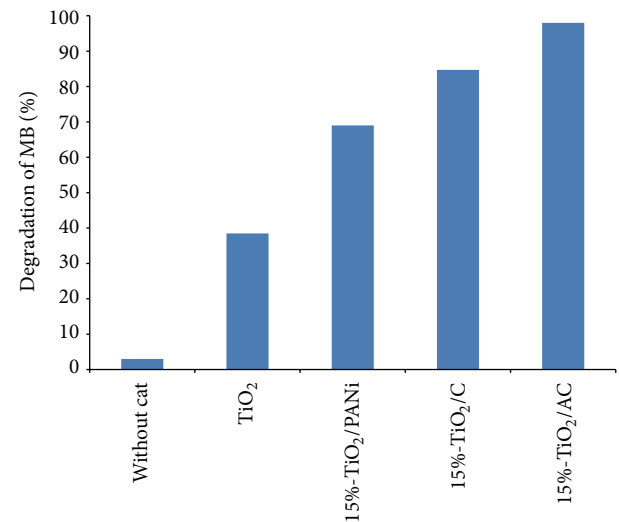


FIGURE 9: Photocatalytic degradation of methylene blue for bare TiO<sub>2</sub>, TiO<sub>2</sub>/PANi, TiO<sub>2</sub>/C, and TiO<sub>2</sub>/AC (0.05 mM MB and 90 min irradiation time).

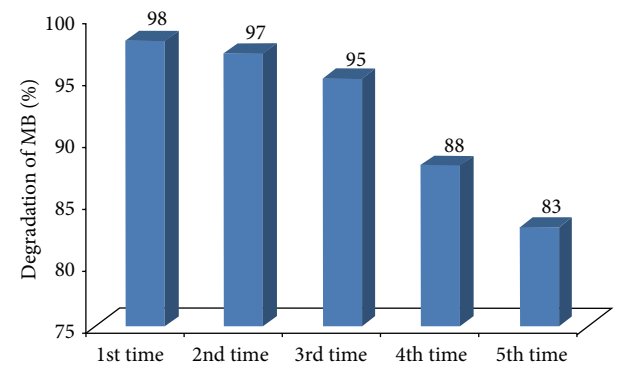


FIGURE 10: Recyclability of TiO<sub>2</sub>/AC was carried out for 5 cycles used.

test demonstrated excellent performance for the synthesized composite.

### Conflict of Interests

The authors declare that there is no conflict of interests regarding the publication of this paper.

### Acknowledgments

The authors would like to acknowledge the financial support of the work by the Universiti Kebangsaan Malaysia for funding this project under the research Grants of Dana Impak Perdana (DLP-2013-015 and FRGS/1/2012/TK07/UKM/3/4) from Ministry of Higher Education (MOHE), Malaysia, and Centre of Research and Innovation Management (CRIM), UKM.

### References

- [1] S. Hussain, Z. Maqbool, S. Ali et al., "Biodecolorization of reactive black-5 by a metal and salt tolerant bacterial strain *Pseudomonas* sp. RA20 isolated from Paharang drain effluents in Pakistan," *Ecotoxicology and Environmental Safety*, vol. 98, pp. 331–338, 2013.
- [2] J. Zhao, C. Chen, and W. Ma, "Photocatalytic degradation of organic pollutants under visible light irradiation," *Topics in Catalysis*, vol. 35, pp. 269–278, 2005.
- [3] D. Bahnemann, "Photocatalytic water treatment: solar energy applications," *Solar Energy*, vol. 77, no. 5, pp. 445–459, 2004.
- [4] U. I. Gaya and A. H. Abdullah, "Heterogeneous photocatalytic degradation of organic contaminants over titanium dioxide: a review of fundamentals, progress and problems," *Journal of Photochemistry and Photobiology C: Photochemistry Reviews*, vol. 9, no. 1, pp. 1–12, 2008.
- [5] M. R. Hoffmann, S. T. Martin, W. Choi, and D. W. Bahnemann, "Environmental applications of semiconductor photocatalysis," *Chemical Reviews*, vol. 95, no. 1, pp. 69–96, 1995.
- [6] O. Carp, C. L. Huisman, and A. Reller, "Photoinduced reactivity of titanium dioxide," *Progress in Solid State Chemistry*, vol. 32, no. 1-2, pp. 33–177, 2004.
- [7] T. Tachikawa, M. Fujitsuka, and T. Majima, "Mechanistic insight into the TiO<sub>2</sub> photocatalytic reactions: design of new photocatalysts," *Journal of Physical Chemistry C*, vol. 111, no. 14, pp. 5259–5275, 2007.
- [8] S. X. Liu, X. Y. Chen, and X. Chen, "A TiO<sub>2</sub>/AC composite photocatalyst with high activity and easy separation prepared by a hydrothermal method," *Journal of Hazardous Materials*, vol. 143, no. 1-2, pp. 257–263, 2007.
- [9] L. F. Velasco, J. B. Parra, and C. O. Ania, "Role of activated carbon features on the photocatalytic degradation of phenol," *Applied Surface Science*, vol. 256, no. 17, pp. 5254–5258, 2010.
- [10] W. N. R. W. Isahak, M. W. M. Hisham, and M. A. Yarmo, "Highly porous carbon materials from biomass by chemical and carbonization method: a comparison study," *Journal of Chemistry*, vol. 2013, Article ID 620346, 6 pages, 2013.
- [11] T. Torimoto, Y. Okawa, N. Takeda, and H. Yoneyama, "Effect of activated carbon content in TiO<sub>2</sub>-loaded activated carbon on photodegradation behaviors of dichloromethane," *Journal of Photochemistry and Photobiology A: Chemistry*, vol. 103, no. 1-2, pp. 153–157, 1997.
- [12] B. Tryba, "Increase of the photocatalytic activity of TiO<sub>2</sub> by carbon and iron modifications," *International Journal of Photoenergy*, vol. 2008, Article ID 721824, 15 pages, 2008.
- [13] J. Matos, J. Laine, and J. Herrmann, "Association of activated carbons of different origins with titania in the photocatalytic purification of water," *Carbon*, vol. 37, no. 11, pp. 1870–1872, 1999.
- [14] J. Araña, J. M. Doña-Rodríguez, E. Tello Rendón et al., "TiO<sub>2</sub> activation by using activated carbon as a support: part I. Surface characterisation and decantability study," *Applied Catalysis B: Environmental*, vol. 44, pp. 161–172, 2003.
- [15] J. Araña, J. M. Doña-Rodríguez, E. Tello Rendón et al., "TiO<sub>2</sub> activation by using activated carbon as a support: part II. Photoreactivity and FTIR study," *Applied Catalysis B: Environmental*, vol. 44, pp. 153–160, 2003.
- [16] S. Brunauer, P. H. Emmett, and E. Teller, "Adsorption of gases in multimolecular layers," *Journal of the American Chemical Society*, vol. 60, no. 2, pp. 309–319, 1938.
- [17] E. P. Barrett, L. G. Joyner, and P. P. Halenda, "The determination of pore volume and area distributions in porous substances. I. Computations from nitrogen isotherms," *Journal of the American Chemical Society*, vol. 73, no. 1, pp. 373–380, 1951.
- [18] G. Liu, T. Wu, J. Zhao, H. Hidaka, and N. Serpone, "Photoassisted degradation of dye pollutants. 8. Irreversible degradation of alizarin red under visible light radiation in air-equilibrated aqueous TiO<sub>2</sub> dispersions," *Environmental Science and Technology*, vol. 33, no. 12, pp. 2081–2087, 1999.
- [19] B. Tryba, A. W. Morawski, and M. Inagaki, "Application of TiO<sub>2</sub>-mounted activated carbon to the removal of phenol from water," *Applied Catalysis B: Environmental*, vol. 41, no. 4, pp. 427–433, 2003.
- [20] J. Ovenstone, "Preparation of novel titania photocatalysts with high activity," *Journal of Materials Science*, vol. 36, no. 6, pp. 1325–1329, 2001.
- [21] J. Moon, H. Takagi, Y. Fujishiro, and M. Awano, "Preparation and characterization of the Sb-doped TiO<sub>2</sub> photocatalysts," *Journal of Materials Science*, vol. 36, no. 4, pp. 949–955, 2001.
- [22] S. S. Arbuj, R. R. Hawaldar, U. P. Mulik, B. N. Wani, D. P. Amalnerkar, and S. B. Waghmode, "Preparation, characterization and photocatalytic activity of TiO<sub>2</sub> towards methylene blue degradation," *Materials Science and Engineering B: Solid-State Materials for Advanced Technology*, vol. 168, no. 1, pp. 90–94, 2010.
- [23] M. Toyoda, Y. Nanbu, Y. Nakazawa, M. Hirano, and M. Inagaki, "Effect of crystallinity of anatase on photoactivity for methyleneblue decomposition in water," *Applied Catalysis B: Environmental*, vol. 49, no. 4, pp. 227–232, 2004.
- [24] R. A. Spurr, "Quantitative analysis of anatase-rutile mixtures with an X-ray diffractometer," *Analytical Chemistry*, vol. 29, no. 5, pp. 760–762, 1957.
- [25] A. H. Elsayed, M. S. Mohy Eldin, A. M. Elsyed, A. H. Abo Elazm, E. M. Younes, and H. A. Motaweh, "Synthesis and properties of polyaniline/ferrites nanocomposites," *International Journal of Electrochemical Science*, vol. 6, no. 1, pp. 206–221, 2011.
- [26] J. Deng, X. Ding, W. Zhang et al., "Magnetic and conducting Fe<sub>3</sub>O<sub>4</sub>-cross-linked polyaniline nanoparticles with core-shell structure," *Polymer*, vol. 43, no. 8, pp. 2179–2184, 2002.
- [27] N. Asim, S. Radiman, and M. A. B. Yarmo, "Preparation and characterization of core-shell polyaniline/V<sub>2</sub>O<sub>5</sub> nanocomposite via microemulsion method," *Materials Letters*, vol. 62, no. 6-7, pp. 1044–1047, 2008.

- [28] S. Lee, Y. Chen, C. Ho, C. Chang, and Y. Hong, "A study on synthesis and characterization of the core-shell materials of  $Mn_{1-x}Zn_xFe_2O_4$ -polyaniline," *Materials Science and Engineering B: Solid-State Materials for Advanced Technology*, vol. 143, no. 1-3, pp. 1-6, 2007.
- [29] R. M. Mohamed, I. A. Mkhaliid, E. S. Baeissa, and M. A. Al-Rayyani, "Photocatalytic degradation of methylene blue by Fe/ZnO/SiO<sub>2</sub> nanoparticles under visiblelight," *Journal of Nanotechnology*, vol. 2012, Article ID 329082, 5 pages, 2012.
- [30] Y. Li, S. Zhang, Q. Yu, and W. Yin, "The effects of activated carbon supports on the structure and properties of TiO<sub>2</sub> nanoparticles prepared by a sol-gel method," *Applied Surface Science*, vol. 253, no. 23, pp. 9254-9258, 2007.
- [31] X. Wang, Z. Hu, Y. Chen, G. Zhao, Y. Liu, and Z. Wen, "A novel approach towards high-performance composite photocatalyst of TiO<sub>2</sub> deposited on activated carbon," *Applied Surface Science*, vol. 255, no. 7, pp. 3953-3958, 2009.
- [32] X. Zhang, M. Zhou, and L. Lei, "Preparation of photocatalytic TiO<sub>2</sub> coatings of nanosized particles on activated carbon by AP-MOCVD," *Carbon*, vol. 43, no. 8, pp. 1700-1708, 2005.
- [33] S. Lubis, L. Yuliati, S. L. Lee, I. Sumpono, and H. Nur, "Improvement of catalytic activity in styrene oxidation of carbon-coated titania by formation of porous carbon layer," *Chemical Engineering Journal*, vol. 209, pp. 486-493, 2012.
- [34] T. Ohno, K. Tokieda, S. Higashida, and M. Matsumura, "Synergism between rutile and anatase TiO<sub>2</sub> particles in photocatalytic oxidation of naphthalene," *Applied Catalysis A: General*, vol. 244, no. 2, pp. 383-391, 2003.
- [35] C. Wu, Y. Yue, X. Deng, W. Hua, and Z. Gao, "Investigation on the synergetic effect between anatase and rutile nanoparticles in gas-phase photocatalytic oxidations," *Catalysis Today*, vol. 93-95, pp. 863-869, 2004.